Electronic and Nuclear Magnetic Resonance Spectroscopic Features of the 1′,4′-Iminopyrimidine Tautomeric Form of Thiamin Diphosphate, a Novel Intermediate on Enzymes Requiring This Coenzyme[†]

Ahmet T. Baykal, Lazaros Kakalis, and Frank Jordan*

Department of Chemistry, Rutgers, the State University, Newark, New Jersey 07102

Received February 27, 2006; Revised Manuscript Received April 18, 2006

ABSTRACT: Appropriate compounds were synthesized to create models for the 1′,4′-imino tautomer of the 4′-aminopyrimidine ring of thiamin diphosphate recently found to exist on the pathway of enzymatic reactions requiring this cofactor [Jordan, F., and Nemeria, N. S. (2005) *Bioorg. Chem. 33*, 190–215]. The N1-methyl-4-aminopyrimidinium compounds synthesized on treatment with a strong base produce the 1,4-imino tautomer whose UV spectrum indicates a maximum between 300 and 320 nm, depending on the absence or presence of a methyl group at the 4-amino nitrogen. The λ_{max} found is in the same wavelength range as the positive circular dichroism band observed on several enzymes and showed a very strong dependence on solvent dielectric constant. To help with the ^{15}N chemical shift assignments, the model compounds were specifically labeled with ^{15}N at the amino nitrogen atom. The chemical shift of the amino nitrogen was deshielded by N1-methylation and then dramatically further deshielded by more than 100 ppm on formation of the 1,4-iminopyrimidine tautomer. Both the UV spectroscopic values and the ^{15}N chemical shift for the 1,4-iminopyrimidine tautomer should serve as useful guides to the assignment of enzyme-bound signals.

The notion that the 4′-aminopyrimidine group of thiamin diphosphate (ThDP)[1] undergoes tautomerization to the 1′,4′-imino form (1′,4′-iminoThDP) during the catalytic cycle of enzymes that utilize it has gained wider acceptance since the appearance of X-ray crystal structural data (*1*). The role and likelihood of tautomerization are suggested by two totally conserved structural features on all ThDP enzymes: (a) the V coenzyme conformation ensuring that the C2 thiazolium atom and the N4′ atom of the 4′-aminopyrimidine ring are within less than 3.5 Å from each other (*2*), potentially enabling the 1′,4′-imino tautomer to participate in proton transfers; and (b) the presence of a glutamate within hydrogen-bonding distance of the N1′ atom of the 4-aminopyrimidine ring, as a potential catalyst for the tautomerization [Scheme 1, as exemplified with the reaction of yeast pyruvate decarboxylase (YPDC)]. As illustrated in the active site structure of YPDC in Figure 1, the residue E51 probably carries out this function (*3*). Chemical evidence for the importance of the 4′-aminopyrimidine moiety of ThDP in
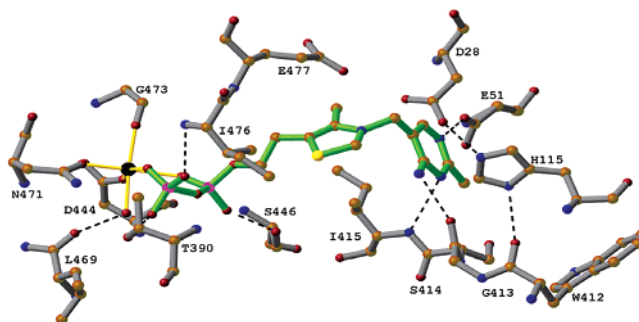

FIGURE 1: Active center structure of YPDC from ref *2*.

catalysis was obtained from ThDP analogues in which one or another nitrogen atom was replaced by carbon (*4*), while a model for activation of the ring for catalysis via tautomerization by N1-protonation was suggested from our laboratories (*5–7*). Notwithstanding the attractive features of this hypothesis, until recently no direct spectroscopic or structural evidence was available on any ThDP enzymes for the presence of the 1′,4′-imino tautomer. In rapid-scan stopped-flow experiments, mixing slow active center variants of YPDC with pyruvate, a UV absorption was noticed with λ_{max} between 300 and 310 nm, shown by circular dichroism (CD) experiments to correspond to a chiral enzyme-bound species (*8*), and demonstrated with model studies to pertain to the 1,4-imino tautomer of 4-aminopyrimidine. Subsequently, the same CD band (and implied tautomer) was clearly observed when mixing methyl acetylphosphonate with either YPDC or the E1 subunit of the *Escherichia coli* pyruvate dehydrogenase complex (PDHc-E1) (*9, 10*) or on reacting methyl benzoylphosphonate with benzoylformate decarboxylase

[1] Abbreviations: ThDP, thiamin diphosphate; YPDC, yeast pyruvate decarboxylase; PDHc-E1, pyruvate dehydrogenase complex E1 subunit; BFD, benzoylformate decarboxylase; CD, circular dichroism; DMSO, dimethyl sulfoxide; NaHMDS, sodium bistrimethylsilylamide; DBU, 1,8-diazabicyclo(5.4.0)undec-7-ene; THF, tetrahydrofuran; TMS, tetramethylsilane; NMR, nuclear magnetic resonance spectroscopy; DEPT, distortionless enhancement by polarization transfer; HSQC, heteronuclear single-quantum correlation; HMBC, heteronuclear multiple bond correlation; COSY, proton–proton correlation spectroscopy; HMQC, heteronuclear multiple-quantum correlation; NOESY, nuclear Overhauser enhancement spectroscopy.

Scheme 1: Mechanism of Pyruvate Decarboxylase

R1 = 4'-amino-2-methyl-5-pyrimidyl
R2 = β-hydroxyethyldiphosphate
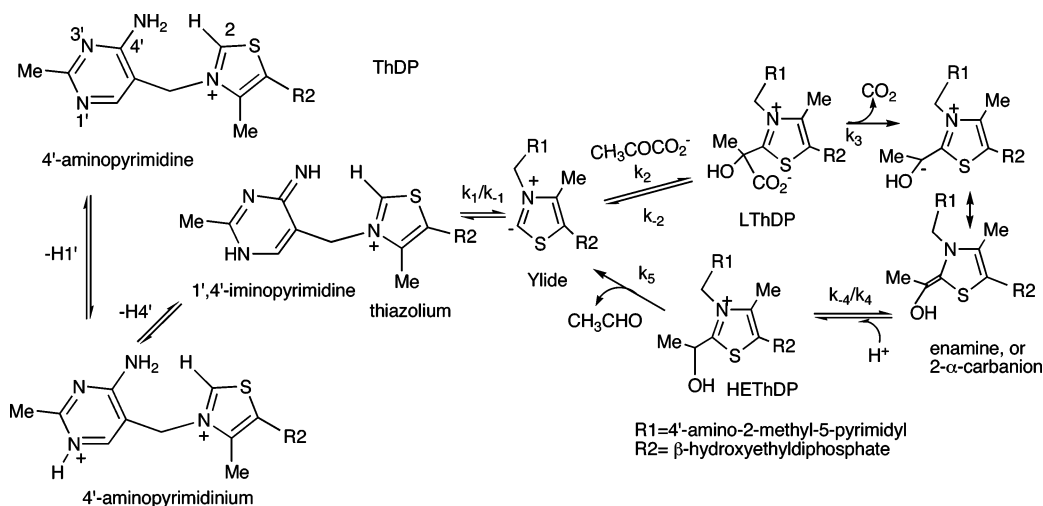
(BFD) (*11*). In these examples, the keto group of the substrate analogue phosphonate forms a covalent adduct with the thiazolium C2 atom of ThDP, an adduct that resembles the predecarboxylation intermediate C2α-lactylthiamin diphosphate (LThDP in Scheme 1) which cannot be decarboxylated. The reaction in each case is signaled by the appearance of a positive circular dichroism (CD) signal in the range of 300−307 nm. Research with a number of YPDC and PDHc-E1 variants prompted us to speculate that the ThDP cofactor exists as the 1′,4′-iminoThDP tautomer with each tetrahedral adduct on the pathway (*10*). Earlier, we had reported preliminary electronic spectroscopic data on chemical models which supported assignment of the positive CD signal at 300−310 nm to the 1,4-imino tautomer (*8*).

Given that there is interest in confirming such findings by other physical methods, such as NMR, on the proteins themselves, one needs to generate models for the chemical shifts.

While both the thiazolium C2H and the 4′-amino group were found in their conventionally written forms in the absence of substrate or analogue on YPDC according to ^{13}C (*3*) and ^{15}N NMR (*12*), respectively, the chemical shifts of the alternatives, of the C2-carbanion or ylide/carbene and of the imino nitrogen atom, need to be known so one can search for them in the spectrum. For example, the chemical shift of the C2 atom is deshielded by nearly 100 ppm [from 155 (*3*) to 253 (*13*) ppm] on loss of a proton. No comparable information is yet available for the change in chemical shift of the N4′ atom on tautomerization. We here report ^{15}N chemical shifts and further UV spectroscopic evidence for models for the 1′,4′-iminoThDP (without the thiazolium diphosphate, whose absence should not significantly alter the conclusions).

As before, we generated the 1,4-iminopyrimidine tautomer of 4-aminopyrimidine by N-methylating the N1 ring nitrogen atom (*6*) and then titrating the amino proton(s) with a base. We learned from such studies that these amino protons present two experimental challenges: (a) they are dissociated in a "concerted" manner; i.e., the UV titration curves for the first and second proton dissociation overlap; and (b) in the NMR studies the attached protons exchange broaden the ^{15}N resonance. To help to interpret both UV spectral and NMR chemical shift assignments, [4-^{15}N]aminopyrimidine

and N4-methyl-[4-^{15}N]aminopyrimidine were synthesized. The results provide strong additional support for the earlier suggested UV λ_{max} values, show that the λ_{max} varies strongly with solvent dielectric constant, and, importantly, reveal a very large chemical shift of the amino nitrogen on conversion of the amino to the imino tautomeric form.

EXPERIMENTAL PROCEDURES

All chemicals used for the synthesis were of the highest quality commercially available and were used without further purification. CD$_3$CN was dried over molecular sieves. The ^1H chemical shifts are reported with respect to tetramethylsilane (0.00 ppm) as an internal standard. UV spectra were recorded on a Varian Cary 300 Bio UV−visible spectrophotometer. Electrospray ionization mass spectrometry (ESI-MS) was carried out on a Thermo Finnigan LCQ Duo mass analyzer.
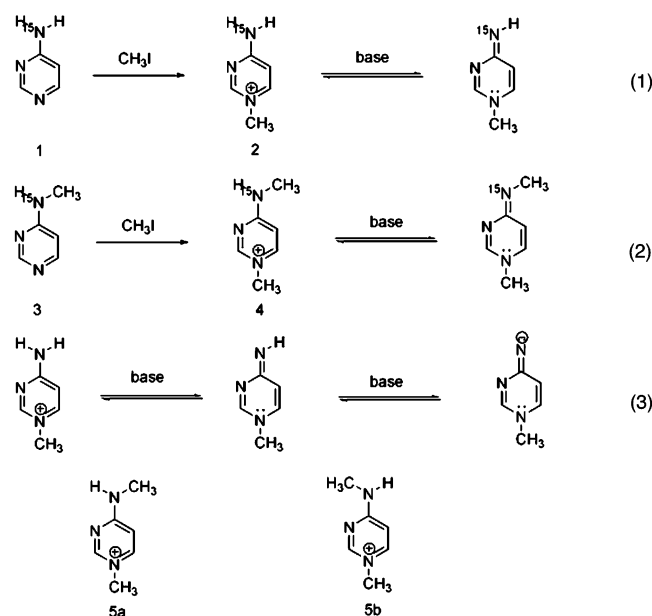
Synthesis of Model Compounds. Both ^{15}N-labeled and unlabeled versions of the various compounds were synthesized; the ^{15}N-labeled starting materials were from Cambridge Isotope Laboratories.

The list of compounds and relevant equations are shown in Scheme 2.

(A) 4-Chloropyrimidine. To phosphorus oxychloride (8.0 mL) at 100 °C was added 4-hydroxypyrimidine (2.0 g) in small portions until dissolution occurred. After 30 min, the solution was cooled and filtered, yielding a yellow precipitate. The yellow precipitate was sublimed at 80 °C under vacuum yielding white needlelike crystals (0.8 g, 40%). The product melted with decomposition over the range of 160−170 °C. ^1H NMR (500 MHz, DMSO-d_6): δ 8.88 (s, 1H), 8.04 (dd, ^3J = 5.5 Hz, ^4J = 1.5 Hz, 1H), 6.55 (d, J = 7.5 Hz, 1H) (*14*).

(B) [4-^{15}N]-4-Aminopyrimidine (1). 4-Chloropyrimidine (281 mg, 2.46 mmol) was added to $^{15}NH_4OH$ (6 N, 5 mL). The mixture was placed in a 160 cm^3 stainless steel Parr pressure reactor. The reactor was heated at 120 °C for 21 h and then cooled to ambient temperature, and the contents were extracted with methanol (2 × 20 mL). The volatiles were removed in vacuo. The crude product was applied to silica and eluted with chloroform−acetone−methanol (70:30:5), yielding the pure product (156 mg, 67%). ^1H NMR (500 MHz, DMSO-d_6): δ 8.31 (t, J = 6.5 Hz, 1H), 8.02 (d,

Scheme 2

FIGURE 2: UV spectrum of compound **2** titrated with DBU in DMSO. Inset: Difference spectra resulting from subtraction of the baseline signal from each spectrum. The difference spectrum has a λ_{max} at 307 nm and is attributed to the corresponding 1,4-imino tautomeric form.

$J = 7.5$ Hz, 1H), 6.39 (d, $J = 7.5$ Hz, 1H), 6.79 (d, $J = 91$ Hz, 2H). ^{13}C NMR (500 MHz, DMSO-d_6): δ 105.1, 154.8, 158.4, 163.3. MS (ESI) 97.1 (M$^+$ + 1) (*15*).

(C) [4-^{15}N]-N1-Methyl-4-aminopyrimidinium Iodide (2). To [4-^{15}N]-4-aminopyrimidine (**1**) (0.1 g, 1.04 mmol) dissolved in 0.5 mL of methanol was added 0.1 mL of methyl iodide. The mixture was refluxed for 2 h and then cooled to room temperature. The volatiles were removed in vacuo, yielding relatively pure product without further purification. ^{1}H NMR (500 MHz, DMSO-d_6): δ 8.71 (t, $J = 6.5$ Hz, 1H), 8.17 (d, $J = 7.5$ Hz, 1H), 6.73 (d, $J = 7.5$ Hz, 1H), 8.92 (d, $J = 90.5$ Hz, 1H), 8.83 (d, $J = 92.5$ Hz, 1H), 3.78 (s, 3H). ^{13}C NMR (500 MHz, DMSO-d_6): δ 37.9, 104.9, 146.8, 154.3, 163.5. MS (ESI): 111.1 (M$^+$), 84, 69 (*8*).

(D) [4-^{15}N]-N4-Methylaminopyrimidine (3). To [^{15}N]-methylamine (960 mg, ~50% ^{15}N) cooled in a 50 mL pressure vessel with liquid nitrogen was added 4-chloropyrimidine (698 mg, 6 mmol). The pressure vessel was warmed to room temperature and after 30 min cooled again to remove the excess methylamine in vacuo. The methylamine hydrochloride side product was removed after neutralization with saturated sodium bicarbonate. The product was repeatedly extracted with methanol. Evaporation of methanol yielded pure product (253 mg, 38%). ^{1}H NMR (500 MHz, DMSO-d_6): δ 8.58 (s, 1H), 8.04 (br, 1H), 6.62 (d, $J = 6.5$ Hz, 1H), 7.79 (qd, $^1J = 92$ Hz, $^2J = 5.5$ Hz, 1H), 2.86 (s, 3H). MS (ESI): 111.1 (M$^+$ + 1), 84, 69.8 (*8*).

(E) [4-^{15}N]-N1,N4-Dimethyl-4-aminopyrimidinium Iodide (4). To [4-^{15}N]-N4-methylaminopyrimidine (**3**) (100 mg, 0.91 mmol) dissolved in 1 mL of methanol was added methyl iodide (100 μL). The mixture was refluxed for 2 h and then cooled to room temperature, and the volatiles were removed in vacuo. The product was pure without further purification. ^{1}H NMR (500 MHz, DMSO-d_6): δ 8.81 (s, 1H), 8.11 (dd, $J = 5.5$ Hz, $^3J = 2$ Hz, 1H), 6.80 (d, $J = 7.5$ Hz, 1H), 9.42 (br, 1H), 2.98 (s, 3H), 3.79 (s, 3H). ^{13}C NMR (500 MHz, DMSO-d_6): δ 27.7, 41.4, 106.0, 145.0, 154.4. MS (ESI): 125.1 (M$^+$), 110.1, 84, 70 (*8*).

(F) N1,N4-Dimethyl-4-aminopyrimidinium Triflate (5). To N4-methylaminopyrimidine (**3**) (70 mg, 0.64 mmol) dis-

solved in 3 mL of chloroform was added methyl trifluoromethanesulfonate (73 μL). The mixture was heated to 80 °C in a 15 mL glass pressure flask for 2 h and then cooled to room temperature, and the volatiles were removed under vacuo. The product crystallized out of the solution. ^{1}H NMR (500 MHz, DMSO-d_6): δ 8.81 (s, 1H), 8.10 (d, $J = 2.0$ Hz, 1H), 6.79 (d, $J = 7.5$ Hz, 1H), 9.38 (br, 1H), 2.98 (d, $J = 5.0$ Hz, 3H), 3.79 (s, 3H) (*8*).

NMR samples were prepared by dissolving the ^{15}N-labeled compounds to estimated final concentrations of 20 mM in 0.7 mL of perdeuterated (99.96 atom % D; Cambridge Isotope Laboratories, Inc.) DMSO-d_6 or CD$_3$CN, also containing 0.1% (v/v) tetramethylsilane (TMS).

One- and two-dimensional NMR spectra were acquired at 25 °C using a Varian INOVA NMR spectrometer (Varian Inc., Palo Alto, CA) operating at a proton frequency of 499.9 MHz and equipped with either a 5 mm triple resonance HCN z-gradient probe or a 5 mm dual broad-band z-gradient probe.

Direct ^{15}N observation was achieved by DEPT (*16*), taking advantage of the 90 Hz one-bond NH coupling of N1-methyl-4-aminopyrimidinium iodide.

Two-dimensional, gradient-selected, one-bond proton–nitrogen correlation spectroscopy (HSQC) (*17–19*), and multiple-bond proton–nitrogen correlation spectroscopy (HMBC) (*20, 21*) were recorded in the phase-sensitive mode (HSQC) or the absolute value mode (HMBC). The HSQC pulse sequence included the TANGO block to suppress signals from N14-coupled protons (*22*) and ^{15}N-decoupling during proton acquisition, using a 2.1 kHz field strength and the GARP decoupling scheme (*23*). The HMBC pulse sequence included a low-pass J filter tuned to exclude one-bond couplings of 90 Hz and to include long-range couplings of 4–5 Hz (*20*); it was acquired without ^{15}N-decoupling to further suppress one-bond coupling cross-peaks.

Typically, 128 t_1 increments of 2K complex data points over 6 kHz (proton) and 50.6 kHz (nitrogen) spectral widths were collected with 8 scans per t_1 increment, preceded by 16 dummy scans, and a relaxation delay of 1–3 s.

Data sets were processed on a Sun Blade 100 workstation (Sun Microsystems Inc., Palo Alto, CA) using the VNMR software package (Varian Inc., Palo Alto, CA). To decrease
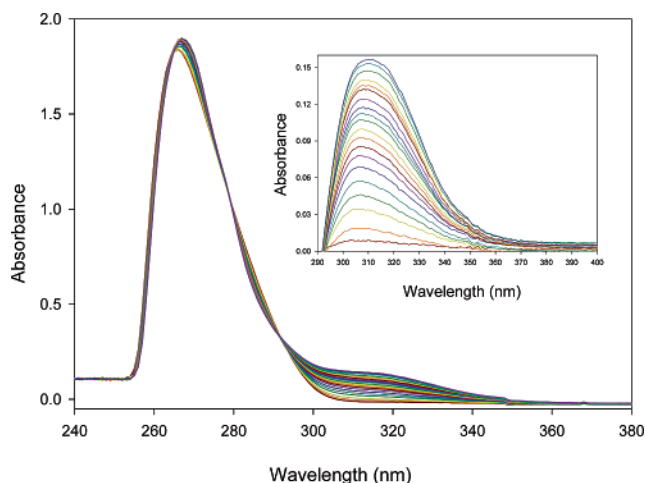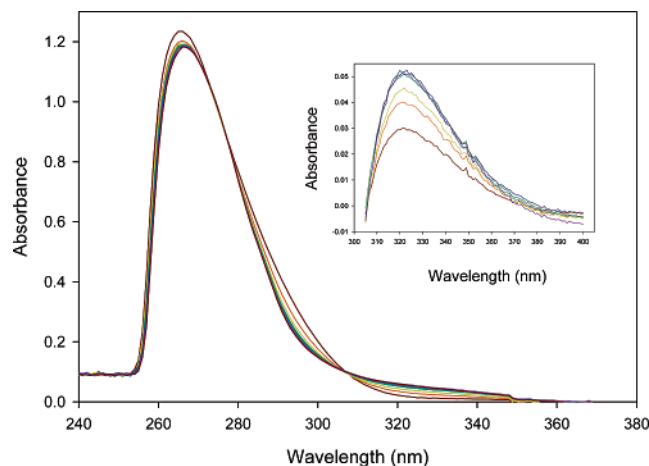
FIGURE 3: UV spectrum of compound **4** titrated with DBU in DMSO. Inset: Difference spectra resulting from subtraction of the baseline signal from each spectrum. The difference spectrum has a λ_{max} at 322 nm and is attributed to the corresponding 1,4-imino tautomeric form.
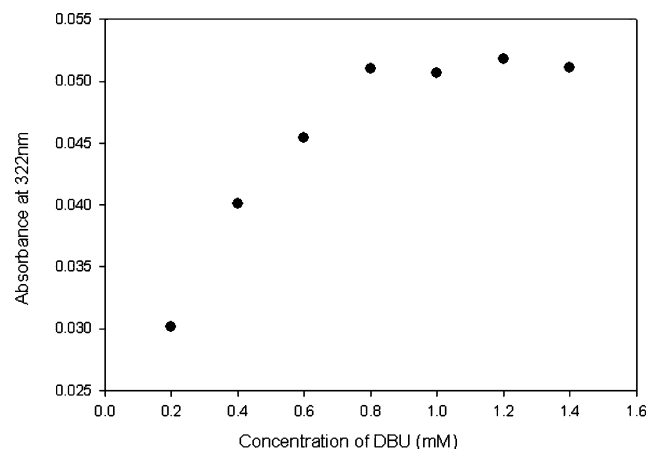

FIGURE 4: Absorbance maximum at 322 nm for 0.08 mM N1,N4-dimethyl-4-aminopyrimidinium iodide (**4**) on addition of DBU in DMSO, resulting in the indicated concentration of DBU.

t_1 ridges arising from incorrect treatment of the first data point in the discrete Fourier transform (FT) algorithm, the spectrum corresponding to the first t_1 value was divided by 2 prior to FT along t_1 (*24*). Shifted (COSY) or unshifted (NOESY, HMQC) Gaussian window functions were used in both dimensions. After forward linear prediction and zero filling in the t_1 dimension, data sets yielded 1K × 1K final matrices.

Proton chemical shifts were referenced vs internal TMS (0.00 ppm). Nitrogen-15 chemical shifts were calculated from the proton chemical shift reference and a ^{15}N τ value of 0.10132912 (*25*, *26*). They are reported vs neat NH_3 (set at 0.00 ppm).

RESULTS

Titration of the Model N1-Methylaminopyrimidinium Salts with Base Monitored by UV Spectroscopy. Abstraction of the amino proton from compound **2** should lead to formation of the 1′,4′-imino tautomer; however, we could not titrate only one of the two amino protons selectively. UV spectroscopy was used to detect formation of the 1,4-iminopyrimidine tautomer, which had an absorbance at 307 nm when DBU was used as the base in DMSO (Figure 2). The
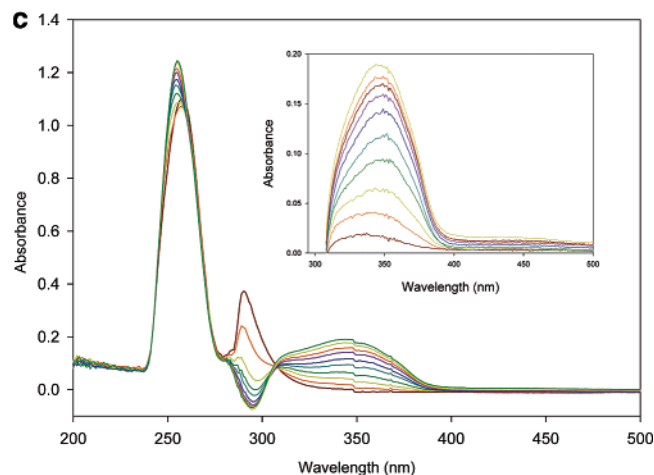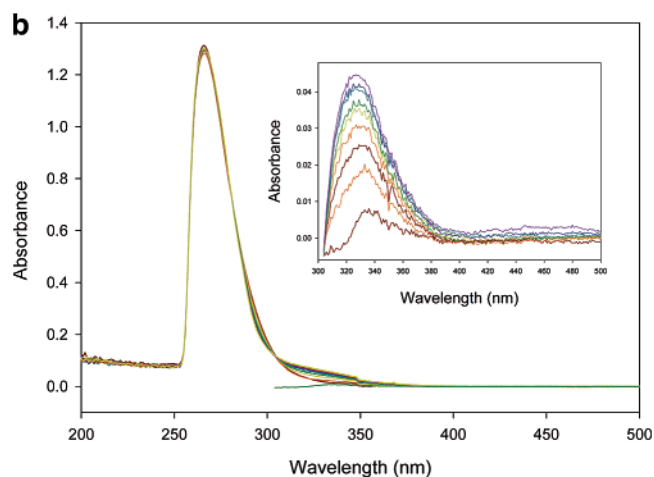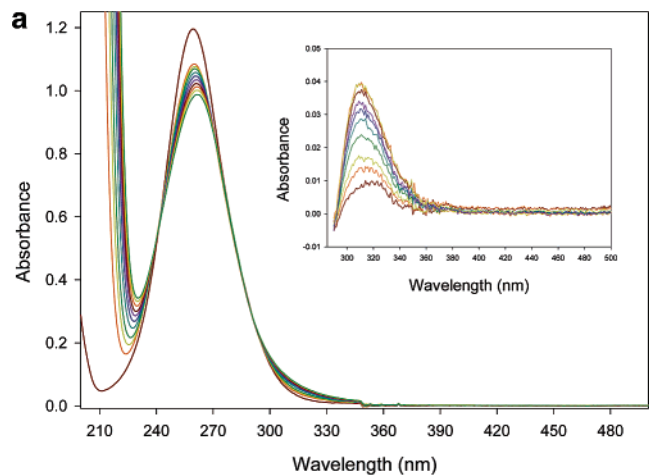

FIGURE 5: (a) UV spectrum of compound **5** titrated with DBU in water. Inset: Difference spectra resulting from subtraction of the baseline signal from each spectrum. The difference spectrum has a λ_{max} at 310 nm and is attributed to the corresponding 1,4-imino tautomeric form. (b) As in (a) but in DMSO. The λ_{max} is at 330 nm. (c) As in (a) but in THF. The λ_{max} is at 350 nm.

absorbance increased continuously as more base was added, making it difficult to draw a clear titration curve that would enable determination of the pK_a of the first amino ionization. The UV−vis spectra revealed the presence of three species since there were two isosbestic points apparent. We believe the compounds produced to be the ones shown in Scheme 2, eq 3. To resolve the issue, N1,N4-dimethyl-4-aminopyrimidinium iodide (**4**) was synthesized, from which only one amino proton could be abstracted. This time, a clearer

Table 1: Proton Chemical Shifts of 4-Aminopyrimidine (**1**), N1-Methyl-4-aminopyrimidinium Iodide (**2**), N4-Methylaminopyrimidine (**3**), N1,N4-Dimethyl-4-aminopyrimidinium Iodide (**4**), and N1,N4-Dimethyl-4-aminopyrimidinium Triflate (**5**)

| | chemical shifts (ppm, vs TMS at 0.00 ppm) | | | | | |
compounds/conditions	C2−H	C5−H	C6−H	N4−CH₃	N1−CH₃	N4−H
1 (DMSO-d_6)	8.31 (t)	6.39 (d)	8.01 (d)	2.86 (s)		6.79 (d)
1 (CD₃CN)	8.47 (t)	6.97 (d)	7.96 (d)	2.84 (d)		5.63 (d)
2 (DMSO-d_6)	8.71 (t)	6.73 (d)	8.17 (d)	2.98 (s)	3.78	8.87 (dd)
2 (CD₃CN)	8.41 (t)	6.51 (d)	8.09 (d)	3.02 (d)	3.80	7.54 (dd)
2 + NaHMDS (CD₃CN)	7.45 (s)	5.82 (d)	6.79 (p)	2.81 (s)	3.46	N/A
3 (DMSO-d_6)	8.59 (s)	6.62 (d)	8.04 (s)	2.98		7.79 (qd)
3 (CD₃CN)	8.41 (s)	6.40 (d)	8.05 (s)	2.93		5.74 (qd)
4 (DMSO-d_6)	8.81 (s)	6.80 (d)	8.11 (dd)	2.98 (s)	3.79 (s)	9.42 (br s)
4 (CD₃CN)	8.50 (s)	6.99 (d)	7.80 (dd)	3.02 (d)	3.77 (s)	8.36 (qd)
4 + NaHMDS (DMSO-d_6)	7.69 (s)	5.65 (d)	6.84 (d)	2.81 (s)	3.25 (s)	N/A
5a (DMSO-d_6)	8.81	6.79	8.10	2.98	3.79	9.38
5b (DMSO-d_6)	8.68	6.92	8.35	2.93	3.79	8.31

titration curve resulted in which the absorbance due to imino tautomer formation levels off (Figure 3), but we needed 10 equiv of base to complete the titration (see Figure 4). Apparently, in DMSO, DBU is a weaker base than the 1,4-iminopyrimidine, enabling a crude estimate of the pK_a for its conjugate acid.

Concerned with the possibility that the iodide counterion may have an effect on the spectra due to the well-known ability of this anion to form charge transfer complexes, compound **5** with the triflate counterion was synthesized. The corresponding 1,4-imino tautomer was generated in three different solvents of differing dielectric constant, and the λ_{max} of the absorption displayed a strong dependence on the dielectric constant: 310 nm in water (Figure 5a; $\epsilon = 80$), 330 nm in DMSO (Figure 5b; $\epsilon = 48$), and 350 nm in THF (Figure 5c; $\epsilon = 7.5$).

NMR Experiments. While initially H₂O/D₂O and NaOH were used for the experiments, due to fast exchange of the amine protons, chemical shifts for the compounds could not be determined. To observe the amino protons, DMSO-d_6 and CD₃CN were used as solvents and sodium bistrimethylsilyl-amide (NaHMDS) as the base. NMR solvents were dried over molecular sieves prior to the experiments because, in the presence of water, the compounds may undergo Dimroth rearrangement (*27*).

Upon methylation of N1, all of the proton chemical shifts moved to more deshielded positions (Table 1). Fast exchange of the amino proton resonance(s) broadens it so it can no longer be observed. Proton abstraction from compound **2** shields all proton chemical shifts.

During the NMR experiments compound **4** still did not yield the proton chemical shift of the 1′,4′-iminopyrimidine exchangeable resonances due to some fast exchange phenomena. Therefore, we synthesized the model compounds **2** and **4** with specific ¹⁵N enrichment at the amino nitrogen positions and used 2D HSQC and HMBC experiments to detect the changes in chemical shifts in the different species. While the one-bond ¹⁵N−H coupling in compound **2** still could not be detected after base abstraction of one amino proton (presumably due to chemical exchange), we succeeded in detecting the chemical shift for the N4 nucleus in the imino tautomeric form generated from compound **4**. As can be seen in Table 2, methylation of the N1 nitrogen of compound **3** deshielded the [¹⁵N]N4 resonance by approximately 25 ppm, a value also confirmed with a 90 Hz DEPT experiment. Base abstraction of the single amino proton from **4** dramatically

Table 2: Nitrogen-15 Chemical Shifts for Compounds **1**−**4**

| | chemical shifts (ppm, vs neat NH₃ at 0.00 ppm) | |
compounds/method/conditions	N4−CH₃	N4−H
1 (HSQC/CD₃CN)		78.01
2 (HSQC/CD₃CN)		103.42
1 (HSQC/ DMSO-d_6)		86.13
2 (HSQC/DMSO-d_6)		110.60
2 + NaHMDS (HSQC/CD₃CN)		N/A
3 (HSQC/CD₃CN)		78.62
4 (HSQC/CD₃CN)		107.86
3 (HSQC/ DMSO-d_6)		78.26
4 (HMBC/DMSO-d_6)	107.28	
4 + NaHMDS (HMBC/DMSO-d_6)	212.09	
4 + NaHMDS (HMBC/CD₃CN)	218.02	
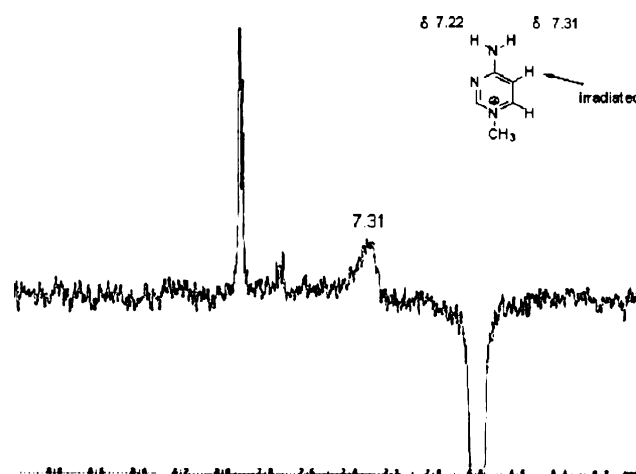
FIGURE 6: Difference ¹H NOE experiment to assign chemically inequivalent amino protons in **2**.

further deshielded the chemical shift of the [¹⁵N]N4 resonance by approximately 105 ppm. On proton abstraction from **4**, there were no more protons left at N4; hence the correlation of the [¹⁵N]N4 nucleus must be via three-bond coupling to the C5H nucleus.

Additionally, we used an NOE difference experiment to differentiate the two amino protons in compound **2**, as shown in Figure 6. The experiment showed that the proton at the N3 side of the amino group has a chemical shift of δ 7.22 ppm while that at the C5 side 7.31 ppm.

DISCUSSION

The UV−vis spectroscopic experiments with the various compounds here reported have given strong support to our

initial report assigning the UV and CD signal between 300 and 310 nm to the 1,4-imino tautomeric form of the 4-aminopyrimidines studied, including that for ThDP on the enzymes. The two consecutive pK_a's for amino deprotonation from compound **2** appear to overlap on addition of base (eq 3 in Scheme 2), making it difficult to obtain a precise single proton titration curve, especially as the spectra of the 1,4-iminopyrimidine tautomer and its N4-deprotonated conjugate base appear to overlap (Figure 2). By N4-methylation leading to **4**, this issue was circumvented, yielding a clean difference spectrum on addition of base (Figure 3) and some approximation of the pK_a of compound **4** for proton loss from the amino group (note that the λ_{max} is shifted to longer wavelength by perhaps 15 nm on N4-methylation). The data in Figure 4 enable us to bracket the pK_a for loss of the sole N4 proton, to be less than one unit higher than of DBU in DMSO. The pK_a for the conjugate acid of DBU in DMSO was quoted between 11 and 12 in one source and 13.9 later (*28*).

The motivation for carrying out experiments in solvents of differing dielectric constant (Figures 5) is that many ThDP enzymes appear to have evolved an active center, which behaves as if it had a low apparent dielectric constant. We tested this notion on both the yeast pyruvate decarboxylase (*29, 30*) and the E1 subunit of the pyruvate dehydrogenase complex from *E. coli* (*31*) by studying the potential stabilization of the central enamine intermediate when approached from either the decarboxylation direction (*30*) or the C2α-hydroxyethylThDP direction (*29, 31*). Our premise for the experiments is that the overall neutral enamine should be stabilized compared to the LThDP or HEThDP on transfer from water (external medium) to a lower dielectric medium (suggested to be provided by the active site). We have also noticed in the CD experiments monitoring the 1′,4′-iminoThDP species that the λ_{max} can vary with the particular enzyme. These model studies now provide the explanation, showing that a lower dielectric constant shifts the λ_{max} to longer wavelength. In a qualitative sense at least, this *is a useful marker for relative hydrophobicity of active centers in ThDP enzymes*. The behavior is consistent with that expected for an n → π* electronic transition.

The ^{1}H chemical shifts did not reveal anything new compared to our previous studies, just emphasizing once more that the ^{1}H chemical shifts become more shielded on amino deprotonation of the N1-alkylpyrimidinium salts. In contrast, the ^{15}N experiments turned out to be remarkably informative, revealing a very large deshielding effect in the 1,4-imino tautomer compared to the amino tautomer, perhaps as large as 130 ppm. It is to be noted that there is precedent for measuring the ^{15}N chemical shift of ThDP on pyruvate decarboxylase from *Zymomonas mobilis*, a study which reported that the chemical shift in the absence of any covalent ThDP-bound intermediate parallels (within 3 ppm) that in solution for free ThDP (*12*). This prompted the authors to conclude that, under their conditions, bound ThDP exists predominantly as the amino tautomer (in comparison with our data on YPDC, we suggest that it is the N1′H+ form). We also suggest that during the reaction cycle this may change and have argued, on the basis of CD evidence, that in all tetrahedral intermediates along the reaction pathway (such as LThDP or HEThDP) the 1′,4′-iminoThDP should represent a significant contribution of the total bound ThDP

(*10*). Our chemical shift values here reported will enable future studies to look for the resonance in the appropriate chemical shift range.

Finally, the NOE experiment in Figure 6 suggests that the amino proton in the N1′H+ form is more acidic on the C5 side, where it presumably is removed to form the 1′,4′-imino tautomer, given that the hydrogen atom on the N3 side is hydrogen bonded in many structures to a backbone carbonyl oxygen atom (see also ref *7*).

REFERENCES

1. Jordan, F., and Nemeria, N. S. (2005) Experimental observation of thiamin diphosphate-bound intermediates on enzymes and mechanistic information derived from these observations, *Bioorg. Chem. 33*, 190−215.
2. Arjunan, P., Umland, T., Dyda, F., Swaminathan, S., Furey, W., Sax, M., Farrenkopf, B., Gao, Y., Zhang, D., and Jordan, F. (1996) Crystal structure of the thiamin diphosphate dependent enzyme pyruvate decarboxylase from the yeast *Saccharomyces cerevisiae* at 2.3Å resolution, *J. Mol. Biol. 256*, 590−600.
3. Kern, D., Kern, G., Neef, H., Tittmann, K., Killenberg-Jabs, M., Wikner, C., Schneider, G., and Hübner, G. (1997) How thiamine diphosphate is activated in enzymes, *Science 275*, 67−70.
4. Schellenberger, A. (1998) Sixty years of thiamin diphosphate biochemistry, *Biochim. Biophys. Acta 1385*, 177−186.
5. Jordan, F., and Mariam, Y. H. (1978) N-1′-Methyl thiamin, a model for the role of the pyrimidine ring in thiamin pyrophosphate requiring enzymatic reactions, *J. Am. Chem. Soc. 100*, 2534−2541.
6. Jordan, F., Chen, G., Nishikawa, S., and Sundoro-Wu B (1982) Potential roles of the aminopyrimidine ring in thiamin catalyzed reactions, *Ann. N.Y. Acad. Sci. 378*, 14−31.
7. Jordan, F. (1982) ^{1}H NMR evidence for high barriers to amino group rotation in 4-aminopyrimidines, including thiamin, at low pH in water, *J. Org. Chem. 47*, 2748−2753.
8. Jordan, F., Zhang, Z., and Sergienko, E. (2002) Spectroscopic evidence for participation of the 1′,4′-imino tautomer of thiamin diphosphate in catalysis by yest pyruvate decarboxylase, *Bioorg. Chem. 30*, 188−198.
9. Jordan, F., Nemeria, N., Zhang, S., Yan, Y., Arjunan, P., and Furey, W. (2003) Dual catalytic apparatus of the thiamin diphosphate coenzyme: acid−base via the 1′,4′-iminopyrimidine tautomer along with its electrophilic role, *J. Am. Chem. Soc. 125*, 12732−12738.
10. Nemeria, N., Baykal, A., Joseph, E., Zhang, S., Yan, Y., Furey, W., and Jordan, F. (2004) Tetrahedral Intermediates in thiamin diphosphate-dependent decarboxylations exist as a 1′,4′-imino tautomeric form of the coenzyme, unlike the Michaelis complex or the free coenzyme, *Biochemistry 43*, 6565−6575.
11. Chakraborty, S., Baykal, A, McLeish, M., Kenyon, G. L., Nemeria, N. S., and Jordan, F. (2006) in preparation.
12. Tittmann, K., Neef, H., Golbik, R., Hübner, G. and Kern, D. (2005) Kinetic control of thiamine diphosphate activation in enzymes studied by proton-nitrogen correlated NMR spectroscopy, *Biochemistry 44*, 8697−8700.
13. Arduengo, A. J., Goerlich, J. R., and Marshall, W. J. (1997) A stable thiazole-2-ylidene and its dimer, *Liebigs Ann./Recl.*, 365−374.
14. Brown, D. J. (1950) Synthesis in the pyrimidine series I. Use of pyrimidinethiols, *J. Soc. Chem. Ind., London, Trans. Commun. 69*, 353−355.
15. Orji, C. C., Michalczyk, R., and Silks, L. A. (1998) Synthesis of 2′-β-deoxy-[8-^{13}C,amino-9-^{15}N]adenosine: unusual annulation conditions to assemble the purine core, *J. Org. Chem. 64*, 4685−4689.
16. Doddrell, D. M., Pegg, D. T., and Bendall, M. R. (1982) Distortionless enhancement of NMR signals by polarization transfer, *J. Magn. Reson. 48*, 323−327.
17. Bodenhausen, G., and Ruben, D. J. (1980) Natural abundance nitrogen-15 NMR by enhanced heteronuclear spectroscopy, *Chem. Phys. Lett. 69*, 185−189.
18. Vuister, G. W., Boelens, R., Kaptein, R., Hurd, R. E., John, B., and Van Zijl, P. C. M. (1991) Gradient-enhanced HMQC and HSQC spectroscopy. Applications to ^{15}N-labeled Mnt repressor, *J. Am. Chem. Soc. 113*, 9688−9690.

19. Bax, A., and Pochapsky, S. S. (1992) Optimized recording of heteronuclear multidimensional NMR spectra using pulsed field gradients, *J. Magn. Reson. 99*, 638−643.

20. Bax, A., and Summers, M. F. (1986) Proton and carbon-13 assignments from sensitivity-enhanced detection of heteronuclear multiple-bond connectivity by 2D multiple quantum NMR, *J. Am. Chem. Soc. 108*, 2093−2094.

21. Willker, W., Leibfritz, D., Kerssebaum, R., and Bermel, W. (1993) Gradient selection in inverse heteronuclear correlation spectroscopy, *Magn. Reson. Chem. 31*, 287−292.

22. Wimperis, S., and Freeman, R. (1984) An excitation sequence which discriminates between direct and long-range CH coupling, *J. Magn. Reson. 58*, 348−353.

23. Shaka, A. J., Barker, P. B., and Freeman, R. (1985) Computer-optimized decoupling scheme for wideband applications and low-level operation, *J. Magn. Reson. 64*, 547−552.

24. Otting, G., Widmer, H., Wagner, G., and Wüthrich, K. (1986) Origin of τ_2 and τ_2 ridges in 2D NMR spectra and procedures for suppression, *J. Magn. Reson. 66*, 187−193.

25. Wishart, D. S., Bigam, C. G., Yao, J., Abildgaard, F., Dyson, H. J., Oldfield, E., Markley, J. L., and Sykes, B. D. (1995) H1, C13 and N15 chemical shift referencing in biomolecular NMR, *J. Biomol. NMR 6*, 135−140.

26. Harris, R. K., Becker, E. D., Cabral de Menezes, S. M., Goodfellow, R., and Granger, P. (2001) Nuclear spin properties and conventions for chemical shifts (IUPAC Recommendations 2001), *Pure Appl. Chem. 73*, 1795−1818.

27. Dimroth, O. (1909) Intramolecular rearrangements, *Ann. 364*, 183−226.

28. Schlesinger, R., Schlemper, H., Hasenfratz, C., Willaredt, J., Dambacher, T., Breuer, T., Ottaway, C., Fletschinger, M., Boele, J., Fritz, H., Putzas, D., Rotter, H. W., Bordwell, F. G., Satish, A. V., Ji, G.-Z., Peters, E.-M., Peters, K., von Schnering, H. G., Walz, L. (1996) Extremely strong, uncharged auxiliary bases. Monomeric and polymer-supported polyaminophosphazenes (P2-P5), *Liebigs Ann. Chem.*, 1055−1081.

29. Jordan, F., Li, H., and Brown, A. (1999) Remarkable stabilization of zwitterionic intermediates may account for a billion-fold rate acceleration by thiamin diphosphate-dependent decarboxylases, *Biochemistry 38*, 6369−6373.

30. Zhang, S., Liu, M., Yan, Y., Zhang, Z., and Jordan, F. (2004) C2α-Lactylthiamin diphosphate is an intermediate on the pathway of thiamin diphosphate-dependent pyruvate decarboxylation: Evidence on enzymes and models, *J. Biol. Chem. 279*, 54312−54318.

31. Zhang, S., Zhou, L., Nemeria, N., Yan, Y., Zhang, Z., Zou, Y., and Jordan, F. (2005) Evidence for dramatic rate acceleration of an C−H bond ionization rate in thiamin diphosphate enzymes by the protein environment, *Biochemistry 44*, 2237−2243.